HAL
archives-ouvertes.fr

# Unified Pairwise Spatial Relations: An Application to Graphical Symbol Retrieval

Santosh K.C., Laurent Wendling, Bart Lamiroy

▶ **To cite this version:**

Santosh K.C., Laurent Wendling, Bart Lamiroy. Unified Pairwise Spatial Relations: An Application to Graphical Symbol Retrieval. Jean-Marc Ogier, Wenyin Liu and Josep Lladós. Graphics Recognition. Achievements, Challenges, and Evolution, 6020, Springer Berlin / Heidelberg, pp.163-174, 2010, Lecture Notes in Computer Science, 978-3-642-13728-0. 10.1007/978-3-642-13728-0_15 . inria-00516724

**HAL Id: inria-00516724**
**https://hal.inria.fr/inria-00516724**

Submitted on 11 Sep 2010

**HAL** is a multi-disciplinary open access archive for the deposit and dissemination of scientific research documents, whether they are published or not. The documents may come from teaching and research institutions in France or abroad, or from public or private research centers.

L'archive ouverte pluridisciplinaire **HAL**, est destinée au dépôt et à la diffusion de documents scientifiques de niveau recherche, publiés ou non, émanant des établissements d'enseignement et de recherche français ou étrangers, des laboratoires publics ou privés.

# Unified Pairwise Spatial Relations: An Application to Graphical Symbol Retrieval

Santosh K. C.[†] and Laurent Wendling[‡] and Bart Lamiroy[♯]

[†]INRIA Nancy-Grand Est, [‡]Nancy Université Henri Poincarr, [♯]Nancy Université
LORIA - Campus Scientifique - BP 239 - 54506 Vandoeuvre-lés-Nancy Cedex, France
First Name.Last Name@loria.fr

**Abstract.** In this paper, we present a novel unifying concept of pairwise spatial relations. We develop two way directional relations with respect to a unique point set, based on topology of the studied objects and thus avoids problems related to erroneous choices of reference objects while preserving symmetry. The method is robust to any type of image configuration since the directional relations are topologically guided. An automatic prototype graphical symbol retrieval is presented in order to establish its expressiveness.

## 1 Introduction

Pairwise spatial relations can greatly ease image understanding, scene analysis and pattern recognition tasks. It has been widely used in many areas such as, GIS understanding [1, 2] – where it is necessary to handle efficiently both inaccurate and vague spatial data –, analyzing architectural documents for automatic recognition [3], graphical drawing understanding from scanned color map documents [4] and defining efficient image retrieval methods [5–7]. However, it is still difficult to organise and obtain spatial relations in an automated way [8, 9].

In general, there is no particular spatial reasoning approach that can adapt to any type of application. They can be either topological [10–13] or directional [14–18] in nature. Further, models are entirely depending on the characteristics of the studied objects as well as specific application driven needs for spatial relations, such as binary or metrical refinement: the level of detail in the expression of spatial predicates such as *Left*, *Right etc.*, varies widely from one application to another [19] as does to the precision of the quantised information. Moreover, the introduction of metric information often gives rise to asymmetry, rendering it subject to erroneous choices of reference objects, which in turn affect the global positioning semantics.

It is possible however, to identify three main levels of information that are involved in spatial relations: topological (that describes neighborhood and incidence e.g. *Dis-Connected, Externally Connected...*), directional (that describes order in space e.g. *Left, Right...*) and metric (e.g. *Near, Far...*). Unlike the existing models that separately treat topological and directional relations, this paper unifies topological and directional information into one descriptor as described

in [8] i.e., *topologically* guided *quantised directional* relation with *symmetry*. This unification does not increase computational time. In addition, our method produces angular coverage over a cycle in $\mathbb{R}^2$ that avoids fluctuations of spatial predicates or other instabilities that may occur even with a small change in the quantised information. Further, we built upon the idea of semantic inverse theory [8] and preserved symmetry by using a unique reference point set instead of selecting an object from a pair. Moreover, this unique reference point set gives a very sound basis for determining metric relations. Currently, this aspect is beyond the scope of the paper.

We organise the rest of the paper as follows. Section 2 provides a literature review of existing methods with their strenghts and shortcomings. The proposed method appears in section 3, immediately followed by an example. Section 4 explores a series of tests. In section 5, a prototype application based on the proposed method is explored. Section 6 concludes the paper along with a few steps to go further.

## 2 Review

Topological relations are invariant to topological transformations [20]. These encompass, but are not restricted to rigid transforms as rotation, scaling, and translation. Since we are interested in developing topologically guided directional relations, we need to assess both topology and directional parts. We distinguish the following topological models: the 4-intersection model [10], the 9-intersection model [11], the Voronoi-based 9-intersection model [21], the general intersection model [22] and the calculus-based model [23]. In this paper, we will be considering the 9-intersection model instead of the 4-intersection [24]. The Voronoi-based 9-intersection model is found to be inappropriate in our context. As mentioned earlier, no existing model fully integrates topology. They rather have various degrees of sensitivty to or awareness of topological relations. The fact is that integrating both high level metrical directional and topologically sound descriptions is computationally expensive. Existing approaches present a trade-off between these factors.

The *cone-shaped* model reduces relative positionning to the discretised angle [17] of the sole centroids. It is robust to small variations of shape and size and separation. However, in cases where the centroids coincide it cannot produce any measure. It even leads to the computation of wrong directions, particularly in the case of concavity, where the centroid does not fall within the shape. Extensions like [25], do not lift such ambiguities, nor does it handle to overlapping regions.

Overlapping is a complex problem and approaches based on *angle histograms* are more efficient. Let two objects $\mathbb{A}$ and $\mathbb{B}$ be considered as the sets of their pixels: $\mathbb{A} = \{a_i\}_{i=1\ldots m}$ and $\mathbb{B} = \{b_j\}_{j=1\ldots n}$. The $m \times n$ pairs of points allow for the computation of a set of angles $\theta_{i,j}$ between each $(a_i, b_j)$. The histogram $H$ representing the frequency of occurrence of each angle $f_\theta$ can then be formulated as $H_\theta(\mathbb{A}, \mathbb{B}) = [\theta, f_\theta]$. Besides a higher time complexity, there is no significant

difference between the *cone-shaped* and the *angle histogram* model when objects are separated by a relatively large distance. The approach was thoroughly studied from its accuracy point of view, and its ambiguity for describing different pairs of objects, resulting in identical histograms [15]. The work was also extended to include metric information in [26], but cannot handle complex objects with holes.

Approaches based on the *Minimum Bounding Rectangle* (MBR) [18, 27, 5, 28, 12] give more interesting relations as they also approximate shape and size of the object. The quality of the bounding rectangle depends on compactness[1] of the tile. The sole information used in the MBR approaches is derived from the geometry of the bounding rectangle from which externally aligned orientations: *Left*, *Right*, *Top* and *Bottom etc.* are straightforwardly derived. There are 36 possible configurations of pairwise spatial relations with MBRs and 218 possible spatial relations between non-empty and connected regions [29]). Further, MBR approximates topological relations, which in turn may express false connection/overlapping.

The *F-Histogram* model gives coherent results [16] at the risk of high processing time. It is generic and depends on a sound mathematical framework. It considers pairs of longitudinal sections instead of pairs of points. It does not cover basic topological relations such as, *Inside* and *Overlap* nor does it integrate metric information. Another well-known approach uses *fuzzy landscapes* [14], and is based on fuzzy morphological operators.

## 3 Proposed Method

In addition to the shortcomings mentioned earlier, proper reference is always a primary factor to organise spatial relations between the objects. It is to be reminded that a change of reference object implies a change in spatial predicates. This, in its turn, may eventually affect overall spatial reasoning (if reference is not given).

In our method, we propose to unify topology and directional relations between the objects $\mathbb{A}$ and $\mathbb{B}$. The proposed method is summarised in two steps. We first extract a unique reference point set $\mathbb{R}$ based on their MBR $(\hat{\mathbb{A}}, \hat{\mathbb{B}})$ topology. This $\mathbb{R}$, thus avoids problems related to erroneous choices of reference entities and will guarantee that subsequent computations of spatial relations $\Re$. In addition, it preserves symmetry.

### 3.1 Unique Reference Point Set $\mathbb{R}$ based on Topology

Fig. 1 shows examples of topological configurations and the corresponding reference region $\mathbb{R}$ that they define. $\mathbb{R}$ is derived from the topological relation between $\hat{\mathbb{A}}$ and $\hat{\mathbb{B}}$, as either the common region of two neighbouring sides in the case of disconnected components or the intersection in the case of overlapping, equal or

[1] Compactness $= \frac{Area(\mathbb{A})}{Area(MBR(\mathbb{A}))}$

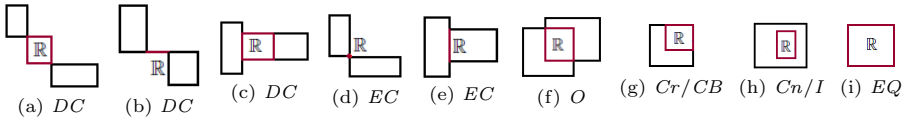


**Fig. 1.** $\mathbb{R}$ via topological relations

otherwise connected components. In what follows we shall use the characteristic points $\mathbb{R}p_i$ (extrema and centroid) of $\mathbb{R}$ as,

$$\mathbb{R} = \{\mathbb{R}p_i\}_{i=1\ldots 2n+1}$$

where $n$ is the dimensionality of the region. The dimension of $\mathbb{R}$ changes with the topological relations (Fig. 1). In this illustration, $\mathbb{R}$ becomes both 1D (b) and 2D (a,c) when two MBRs are *Dis-Connected* (*DC*) while, 0D (d) and 1D (e) when they are *Externally Connected* (*EC*). Similarly, only 2D (f, g, h, i) when *Overlap*ping (*O*), *Cover/Covered By* (*Cr*/*CB*), *Contain/Inside* (*Cn*/*I*), and *Equal* (*EQ*) occur. These are the basic topological predicates closely related to human understanding in conncetion with the Region Connection Calculus-8 (RCC-8) [13]. We express the topological relations in a 9-dimensional binary space based on the 9-intersection model [11]. It uses on the intersections of the boundaries ($\partial*$), interiors ($*^o$) and exteriors ($*^-$) of two shapes $\mathbb{A}$ and $\mathbb{B}$. The topological configuration $Topo.(\mathbb{A},\mathbb{B})$ is a vector in this space in which componetns equal 0 if the corresponding intersection is empty, and 1 otherwise, as shown here:

$$Topo.(\mathbb{A},\mathbb{B}) = \begin{bmatrix} \mathbb{A}^o \cap \mathbb{B}^o & \mathbb{A}^o \cap \partial\mathbb{B} & \mathbb{A}^o \cap \mathbb{B}^- \\ \partial\mathbb{A} \cap \mathbb{B}^o & \partial\mathbb{A} \cap \partial\mathbb{B} & \partial\mathbb{A} \cap \mathbb{B}^- \\ \mathbb{A}^- \cap \mathbb{B}^o & \mathbb{A}^- \cap \partial\mathbb{B} & \mathbb{A}^- \cap \mathbb{B}^- \end{bmatrix}$$

Therefore $3 \times 3$ binary signature for $DC(\mathbb{A},\mathbb{B}) = \left[\begin{smallmatrix} 0 & 0 & 1 \\ 0 & 0 & 1 \\ 1 & 1 & 1 \end{smallmatrix}\right]$, $EC(\mathbb{A},\mathbb{B}) = \left[\begin{smallmatrix} 0 & 0 & 1 \\ 0 & 1 & 1 \\ 1 & 1 & 1 \end{smallmatrix}\right]$, $\ldots$, $EQ(\mathbb{A},\mathbb{B}) = \left[\begin{smallmatrix} 1 & 0 & 0 \\ 0 & 1 & 0 \\ 0 & 0 & 1 \end{smallmatrix}\right]$.

### 3.2 Directional Relations - Radial Line Model (RLM)

The model precisely yields angular coverage over a cycle in $\mathbb{R}^2$ and thus avoids the use of spatial predicates as in the existing models. It is to remind that the level of expresion of spatial predicates is sensitive to every small change in quantised information. The model further, explores both qualitative and quantitative process.

**Binary Relations** Let $\mathbb{X}$ be one of the initial objects $\mathbb{A}$ or $\mathbb{B}$ and let their reference region be $\mathbb{R}$. At every $\mathbb{R}p_i$, we cover the surrounding space at regular radial intervals of $\Theta = 2\pi/m$, such that $\theta_j = j\Theta$. It rotates over a cycle and

intersecting with $\mathbb{X}$, and generates binary values at every step of its rotation (Fig. 2). This gives a boolean histogram of angular coverage,

$$\mathcal{H}(\mathbb{X}, \mathbb{R}p_i) = [I(\mathbb{R}p_i, j\Theta)]_{j=0..m} \text{ where } I(\mathbb{R}p_i, \theta_j) = \begin{cases} 1 \text{ if } line(\mathbb{R}p_i, \theta_j) \cap \mathbb{X} \neq \emptyset \\ 0 \text{ otherwise} \end{cases}$$

This is extended *wlog* to the sector defined by two successive angle values: $Cone(\mathbb{R}p_i, \theta_j, \theta_{j+1})$. The process is repeated for every $\mathbb{R}p_i$.

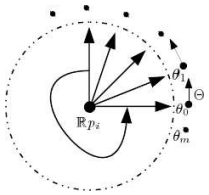


**Fig. 2.** Radial line $line(\mathbb{R}p_i, \theta_j)$ rotation

**Refined Relations** In order to be robust to noise and to border conditions due to discritization, we extend the boolean description by partially building on the cloud model [30]. We normalise the coverage with respect to the total area of the object under consideration with respect to every $\mathbb{R}p_i$, $\frac{Area(Cone(\mathbb{R}p_i, \theta_j, \theta_{j+1}))}{Area(\mathbb{X})}$ such that $\sum \mathcal{H}(.) = 1$. This goes without loss of generality and it is robust to any type of point set (either a point, a line or a region). It is not only convey information about the presence of objects in a given direction, but also infores about the proportion of the object that is lying there.

We average the resulting histograms (from every $\mathbb{R}p_i$) to produce $\Re(\mathbb{X}, \mathbb{R})$.

**Remarks**

- Spatial Relations: We use $\Re_{Bin}(.)$ and $\Re_{Ref}(.)$ for binary and refined relations respectively.
- Symmetry: Due to $\mathbb{R}$, RLM yields two way directional relations as well as it preserves symmetry. For symmetry reasons, we use $\Re(\star, *) = \{\mathcal{H}(\star, \mathbb{R}), \mathcal{H}(*, \mathbb{R})\}$. This guarantees that, $\Re(\star, *) = \Re(*, \star)$.
- Resolution: $\Theta$ determines a trade-off between precision and time complexity, determining *resolution* of $\mathcal{H}$. Smaller the *resolution*, better the information exploitation.

### 3.3 An Example

Fig. 3 shows an example illustrating our method for a pair of truly overlapping objects. We first show how to determine $\mathbb{R}$ from $Topo.(\hat{\mathbb{A}},\hat{\mathbb{B}})$. Fig. 4 shows how both boolean and metrical refinement histograms are produced from $Topo.(\mathbb{R}, \mathbb{X})$.

As an example, we use $\Theta = \pi/20$ to produce $\mathcal{H}$ for $\Re_{Bin}(.)$ and $\Re_{Ref}(.)$. For every $\mathbb{R}p_i$, the visual representations of binary (blue) and refined (red in blue mask – zoomed $\times 3$) histograms are shown for object $\mathbb{A}$ and $\mathbb{B}$ in Fig. 4. For easier understanding, the directional relation signatures with respect to the reference centroid point $\mathbb{R}p_c$ are:

$$\mathcal{H}_{Bin}(\mathbb{A}, \mathbb{R}p_c) = [0\ 0\ 0\ 0\ 0\ 0\ 1\ 1\ 1\ 1\ 1\ 1\ 1\ 1\ 1\ 1\ 0\ 0\ 0\ 0\ 0\ 0\ 0\ 0\ 0\ 0\ 0\ 0]$$
$$\mathcal{H}_{Ref}(\mathbb{A}, \mathbb{R}p_c) = [0\ 0\ 0\ 0\ 0\ 0\ 0.0261\ 0.0722\ 0.0746\ 0.0775\ 0.0708\ 0.0746\ 0.0841$$
$$0.0675\ 0.0433\ 0.0299\ 0.0328\ 0.0323\ 0.0328\ 0.0352\ 0.0299\ 0.0328$$
$$0.0323\ 0.0328\ 0.0352\ 0.0375\ 0.0361\ 0.0095\ 0\ 0\ 0\ 0\ 0\ 0\ 0\ 0\ 0\ 0\ 0]$$

After averaging, it is found that $\Re(\mathbb{A}, \mathbb{R}) \neq \emptyset$ while $\Re(\mathbb{B}, \mathbb{R})$ is. It is due to the fact that $Cr(\mathbb{R}, \mathbb{X})$ or $CB(\mathbb{X}, \mathbb{R})$.

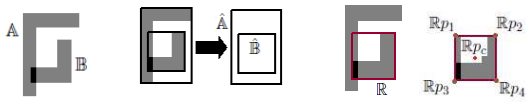


(a) A pair (b) Encased with MBR (c) $\mathbb{R}$ generation

**Fig. 3.** An example to illustrate the proposed method (a truly overlapping case)

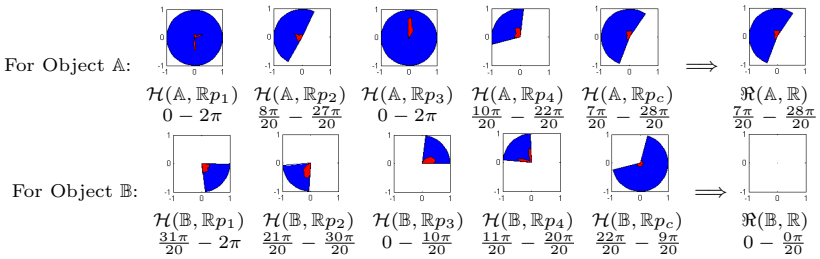


**Fig. 4.** $\frac{7\pi}{20} - \frac{28\pi}{20}(\mathbb{A}, \mathbb{R})$ ($1^{st}$ row) and $0 - \frac{0\pi}{20}(\mathbb{B}, \mathbb{R})$ ($2^{nd}$ row)

## 4 Experiments

In this experiment, we use segmented and labeled objects in order just to explore the expressive power of the method. Table. 1 shows the behaviour of our method on a series of objects, ranging from simple, solid and regular pairs of objects to concave, as well as complex ones, covering all possible topologies. The overall result shows a comparison between the topology of the shapes themselves $(\mathbb{A}, \mathbb{B})$ as well as their MBR $(\hat{\mathbb{A}}, \hat{\mathbb{B}})$. Comparison made with the topology between them determines the qualtity of the MBR tile. The difference in topological relations

is due to MBR false connection/overlapping. It is however, not a problem in our method since it uses the initial objects $(\mathbb{A}, \mathbb{B})$ to produce $\Re$ after the discovery of $\mathbb{R}$. Further, $\Re_{Bin}$ and $\Re_{Ref}$ of both objects with respect to $\mathbb{R}$ are also shown in Table 1.

**Table 1.** A series of tests $(\Theta = \frac{\pi}{20})$

| Image with $\mathbb{R}$ | Topology $(\mathbb{A},\mathbb{B})$ | Topology $(\hat{\mathbb{A}},\hat{\mathbb{B}})$ | $\Re_{Bin}(.) + \Re_{Ref}(.)$ $\Re(\mathbb{A},\mathbb{R})$ | $\Re(\mathbb{B},\mathbb{R})$ | Image with $\mathbb{R}$ | Topology $(\mathbb{A},\mathbb{B})$ | Topology $(\hat{\mathbb{A}},\hat{\mathbb{B}})$ | $\Re_{Bin}(.) + \Re_{Ref}(.)$ $\Re(\mathbb{A},\mathbb{R})$ | $\Re(\mathbb{B},\mathbb{R})$ |
|---|---|---|---|---|---|---|---|---|---|
| **Experiment I** | | | | | | | | | |
| (a) | $DC$ | $DC$ | $\frac{11\pi}{20} - \frac{28\pi}{20}$ | $\frac{33\pi}{20} - \frac{8\pi}{20}$ | (d) | $DC$ | $DC$ | $\frac{11\pi}{20} - \frac{28\pi}{20}$ | $\frac{33\pi}{20} - \frac{8\pi}{20}$ |
| (b) | $DC$ | $DC$ | $\frac{11\pi}{20} - \frac{28\pi}{20}$ | $\frac{33\pi}{20} - \frac{8\pi}{20}$ | (e) | $DC$ | $DC$ | $\frac{14\pi}{20} - \frac{28\pi}{20}$ | $\frac{33\pi}{20} - \frac{2\pi}{20}$ |
| (c) | $DC$ | $DC$ | $\frac{11\pi}{20} - \frac{28\pi}{20}$ | $\frac{33\pi}{20} - \frac{8\pi}{20}$ | (f) | $DC$ | $DC$ | $\frac{14\pi}{20} - \frac{28\pi}{20}$ | $\frac{33\pi}{20} - \frac{2\pi}{20}$ |
| **Experiment II** | | | | | | | | | |
| (i) | $DC$ | $DC$ | $\frac{11\pi}{20} - \frac{30\pi}{20}$ | $\frac{33\pi}{20} - \frac{7\pi}{20}$ | (iv) | $DC$ | $Cn$ | $\frac{04\pi}{20} - \frac{37\pi}{20}$ | $0 - \frac{0\pi}{20}$ |
| (ii) | $DC$ | $O$ | $\frac{11\pi}{10} - \frac{31\pi}{20}$ | $\frac{31\pi}{20} - \frac{10\pi}{20}$ | (v) | $DC$ | $Cn$ | $\frac{02\pi}{20} - \frac{39\pi}{20}$ | $0 - \frac{0\pi}{20}$ |
| (iii) | $DC$ | $Cn$ | $\frac{09\pi}{20} - \frac{32\pi}{20}$ | $0 - \frac{0\pi}{20}$ | (vi) | $DC$ | $Cn$ | $0 - \frac{40\pi}{20}$ | $0 - \frac{0\pi}{20}$ |

### 4.1 Discussions

In a few congurations (Table 1), RLM yields identical $\Re_{Bin}$ but different $\Re_{Ref}$ between different pairs of objects. This behaviour can be observed in Experiment I for (a), (b), (c) and (d) as well as (e) and (f). It is to be noted that $\Re_{Ref}$ is only used to cross validate when $\Re_{Bin}$ is found to be non discriminant. Experiment II shows the behaviour of our method on progressive coverage of one object by another. In this illustration, a progressive angular coverage as well as effect of *inclusion* topological relations on directional relations are clearly demonstrated. As in Fig. 4 $\Re(\mathbb{B},\mathbb{R}) = \emptyset$ because $Cn(\mathbb{R},\mathbb{B})$.

Overall, directional relations are topologically guided. For $DC$, $EC$ and $O$ relations, it is straightforward. But for all *inclusion* relations like $Cr/CB$, $Cn/I$,

and $EQ$, $\mathcal{H}(\mathbb{X}, \mathbb{R}) = \emptyset$. Therefore, only one part of $\Re$ needs to be computed. This eventually reduces time complexity as RLM gives no measure.

### 4.2 Time Complexity

In this section we analyse the time complexity behaviour both with respect to the precision ($\Theta$) and the size of the objects. Unlike the existing models described in section 2, processing time does not increase exponentially with the size of the images but has only a little effect. Fig. 5 shows time complexity measure by increasing the size of the image (scaling step +0.2). Overall, the RLM takes almost the same time to make a complete rotation over a cycle in all size of images. This is the main reason for the time complexity graph being approximately level. In order to increase the speed, one can use boundaries of objects to compute the boolean histogram.

It has no doubt that cone shaped and classical projection models run faster than the RLM and histogram of angles (and its variant). In our method, resolution $\Theta$ determines which one to trade off: either quality or computational load. It is to be noted that the RLM resolution should be chosen based on the size of objects under consideration. Further, time complexity is compensated to $\frac{n(n-1)}{2}$ for $n$ objects due to the symmetry relations.

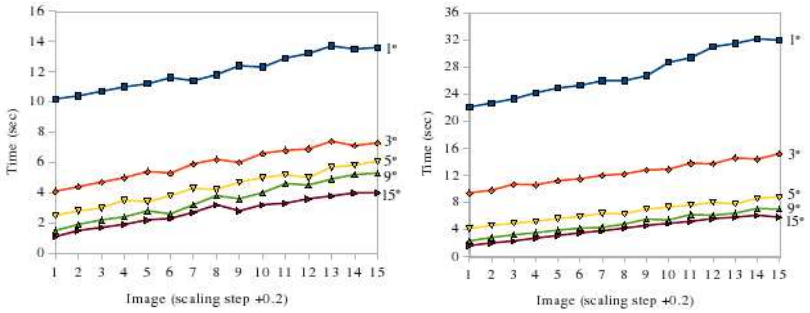


**Fig. 5.** Time complexity for $\Re_{Bin}$ (left) and $\Re_{Ref}$ (right) for a number of different resolutions

## 5 An Application

### 5.1 Symbol Description via Spatial Relations

We use the visual vocabulary presented in [31, 32] to organise spatial relations and use them for symbol description. In our case, the vocabulary consists of: *circles, corners, loose ends* and *thick* (filled) components. To handle arbitrary

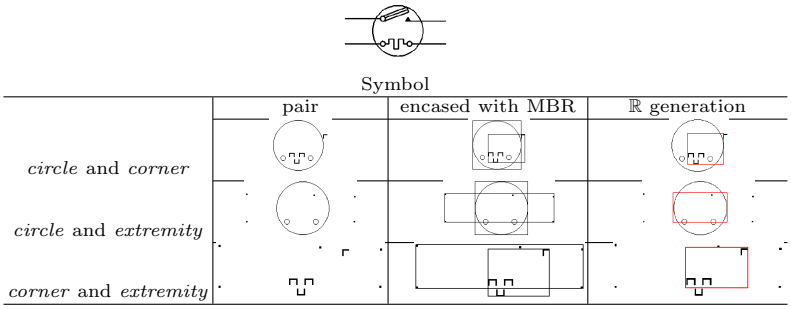


**Fig. 6.** Reference point set $\mathbb{R}$ generation for all possible pairs of classes

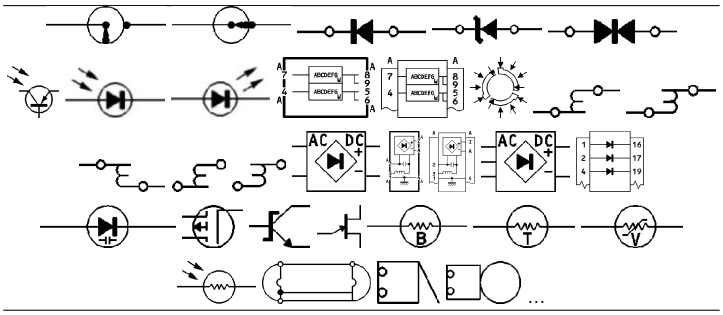


**Fig. 7.** A small set of electrical symbols

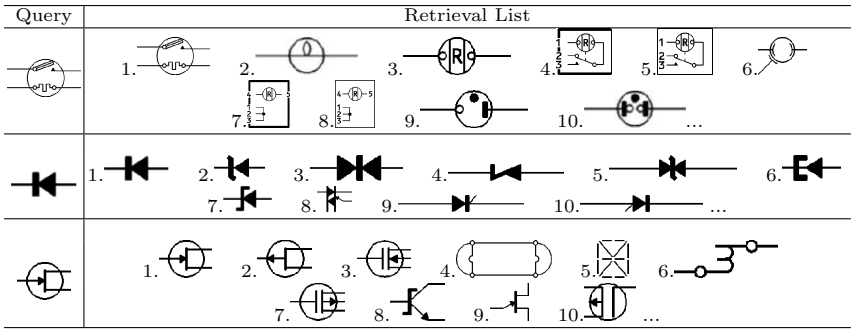


**Fig. 8.** Retrieval lists based on similarity for a few chosen queries $(\Theta = \frac{\pi}{180})$

number of vocabulary elements, we group them together into 'classes' having the same type, as shown in Fig. 6. The symbol is then modeled as a graph in which each group is a typed node, and the arcs, representing the spatial relations $\Re$.

### 5.2 Symbol Retrieval

We use straightforward graph matching to retrieve similar symbols with respect to the chosen query. We manually choose query symbols which are matched with symbols in the database. We employ similarity ranking based on the geometric distance. We take manhattan distance metric between the corresponding relations in the graphs, $\sum_i^n |(\Re_i(.) - \Re'_i(.))|$. Fusion of matching scores from individual relations reflects how similar the symbol in the database with query symbol. Based on the similarity value, we rank retrieval symbols.

Since it is a protype application, we use small database and a few test queries. A sample of the database is shown in Fig. 7. Ranking retrieval lists for a few choosen queries are shown in Fig. 8.

## 6 Conclusions and Further Works

In this paper, we have presented a new concept of unifying pairwise spatial relations. Since directional relations are topologically guided, one does not need to model them separately. The method provides accurate spatial organisation for any type of image configuration. In addition, it produces symmetric directional relations thanks to the use of a unique reference point set. These two way spatial relations are developed at one pass, while this is not the case in existing models.

One of the possible applications – prototype symbol retrieval – is reported, using a small database. Further work consists of using intra-class spatial relations as well as pre-filtering techniques to establish precision and recall in symbol retrieval. We will further develop the use of this method for scene matching and image analysis tasks which will ultimately bring it into the context of full image recognition.

## References


1. Worboys, M.: GIS - A computing perspective. Taylor and Francis (1995)
2. Goodchild, M., Gopal, S.: The Accuracy of Spatial Databases. Taylor and Francis, Basingstoke, UK (1990)
3. Vandenbrande, J.H., Requicha, A.A.G.: Spatial Reasoning for the Automatic Recognition of Machinable Features in Solid Models. IEEE PAMI **15**(12) (December 1993) 1269–1285
4. Centeno, J.S.: Segmentation of Thematic Maps Using Colour and Spatial Attributes. In Tombre, K., Chhabra, A.K., eds.: Graphics Recognition—Algorithms and Systems. Volume 1389 of LNCS. Springer-Verlag (1998) 221–230
5. Lee, S.H., Hsu, F.J.: Spatial Reasoning and Similarity Retrieval of Images Using 2D C-string Knowledge Representation. PR **25**(3) (1992) 305–318
6. Heidemann, G.: Combining spatial and colour information for content based image retrieval. CVIU **94** (2004) 234–270
7. Medasani, S., Krishnapuram, R.: A fuzzy approach to content-based image retrieval. In: Proc. of FUZZ-IEEE, Seoul, Korea. (1997) 1251–1260
8. Freeman, J.: The modelling of spatial relations. CGIP **4** (1975) 156–171

9. Rosenfeld, A., Kak, A.: Digital picture processing. Volume 2. Academic Press (1982)
10. Egenhofer, M., Franzosa, R.: Point-set Topological Spatial Relations. Intl. Journal of GIS **5**(2) (1991) 161–174
11. Egenhofer, M., Herring, J.R.: Categorizing Binary Topological Relations Between Regions, Lines, and Points in Geographic Databases. In: Univ. of Maine, Research Report. (1991)
12. Papadias, D., Sellis, T., Theodoridis, Y., Egenhofer, M.J.: Topological Relations in the world of Minimum Bounding Rectangles: a Study with R-trees. In: Intl. Conf. on Managament Data. (1995) 92–103
13. Renz, J., Nebel, B.: Spatial Reasoning with Topological Information. In: Spatial Cogn., An Interdisciplinary Approach to Representing and Processing Spatial Knowledge. Volume 1404 of LNCS. Springer-Verlag (1998) 351–372
14. Bloch, I.: Fuzzy relative position between objects in image processing: a morphological approach. IEEE PAMI **21**(7) (1999) 657–664
15. Wang, X., Keller, J.: Human-Based Spatial Relationship Generalization Through Neural/Fuzzy Approaches. Fuzzy Sets and Systems **101** (1999) 5–20
16. Matsakis, P., Wendling, L.: A New Way to Represent the Relative Position Between Areal Objects. IEEE PAMI **21**(7) (1999) 634–643
17. Mitra, D.: A Class of Star-Algebras for Point-Based Qualitative Reasoning in Two-Dimensional Space. In: 15th Intl. Florida AI Research Society Conf. (2002) 486–491
18. Peuquet, D., CI-Xiang, Z.: An algorithm to determine the directional relationship between arbitrarily-shaped polygons in the plane. PR **20**(1) (1987) 65–74
19. Retz-Schmidt, G.: Various Views on Spatial Prepositions. AI Magazine (1988) 95–104
20. Egenhofer, M.J.: A Formal Definition of Binary Topological Relationships. In: 3rd Intl. Conf. on Foundations of Data Organization and Algorithms, LNCS. (1989) 457–472
21. Chen, J., Li, C., Li, Z., Gold, C.: A Voronoi-based 9-intersection Model for Spatial Relations. Intl. Journal of GISc. **15**(3) (2001) 201–220
22. Abdelmoty, A., El-Geresy, B.: A General Method for Spatial Reasoning in Spatial Databases. In: 4th Intl. Conf. on Information and knowledge Management. (1995) 312–317
23. Clementini, E., Felice, P.D., van Oosterom, P.: A small set of formal topological relationships suitable for end-user interaction. SSD'93, Advances in Spatial Database, Springer LNCS 692 (1993) 277–336
24. Egenhofer, M., Sharma, J., Mark, D.: A Critical Comparison of the 4-Intersection and 9-Intersection Models for Spatial Relations: Formal Analysis. In: In: R. McMaster and M. Armstrong (Eds.). (1993) 56–69
25. Miyajima, K., Ralescu, A.: Spatial Organization in 2D Segmented Images: Representation and Recognition of Primitive Spatial Relations. Fuzzy Sets and Systems **2**(65) (1994) 225–236
26. Wang, Y., Makedon, F.: R-histogram: Quantitative representation of spatial relations for similarity-based image retrieval. In: 11th Annual ACM International Conf. on Multimedia. (2003) 323–326
27. Dutta, S.: Approximate spatial reasoning: integrating qualitative and quantitative constraints. Intl. Journal of Approximate Reasoning **5** (1991) 307–331
28. E.Jungert: Qualitative spatial reasoning for determination of object relations using symbolic interval projections. In: IEEE Sympo. on Visual Lang. (1993) 24–27

29. Sun, H., Chen, X.: Research on Technologies of Spatial Configuration Information Retrieval. In: IEEE 8th ACIS Intl. Conf. on Software Engineering, AI, Networking, and Parallel/Distributed Computing. (2007) 396–401
30. Xuehua, T., Lingkui, M., Kun, Q.: Study on the Uncertain Directional Relations Model based on Cloud Model. In: Intl. Archives of the Photogrammetry, Remote Sensing and Spatial Info. Sc. (2008) 345–350
31. Santosh, K.C., Lamiroy, B., Ropers, J.P.: Utilisation de Programmation Logique Inductive pour la Reconnaissance de Symboles. In: 9èmes Journées Francophones Extraction et Gestion des Connaissances. (2009) 35–42
32. Santosh, K.C., Lamiroy, B., Ropers, J.P.: Inductive logic programming for symbol recognition. In: 10th ICDAR, Barcelona(Spain). (2009) 1330–1334